

## Research Article

# Selection of Optimal Threshold of Generalised Rock Quality Designation Based on Modified Blockiness Index

Qingfa Chen <sup>1,2</sup>, Tingchang Yin <sup>1,2</sup> and Hangyu Jia <sup>3</sup>

<sup>1</sup>College of Resources, Environment and Materials, Guangxi University, Nanning, Guangxi 530004, China

<sup>2</sup>State Key Laboratory of Geomechanics and Geotechnical Engineering, Institute of Rock and Soil Mechanics, Chinese Academy of Sciences, Wuhan 430071, China

<sup>3</sup>School of Resources and Safety Engineering, Central South University, Changsha 410083, China

Correspondence should be addressed to Qingfa Chen; [chenqf@gxu.edu.cn](mailto:chenqf@gxu.edu.cn)

Received 15 October 2018; Accepted 11 December 2018; Published 10 January 2019

Academic Editor: Jian Ji

Copyright © 2019 Qingfa Chen et al. This is an open access article distributed under the Creative Commons Attribution License, which permits unrestricted use, distribution, and reproduction in any medium, provided the original work is properly cited.

Rock quality designation (RQD) is a critical index for quantifying the degree of rock mass jointing; it is widely used for evaluating the qualities and stabilities of engineering rock masses. However, the use of traditional RQD may yield inaccurate assessments because only core pieces longer than 100 mm are counted. To enhance the utility of RQD, generalised RQD was introduced. Based on the modified blockiness index ( $MB_i$ ), the determination of the optimal threshold of generalised RQD was performed. In this work, 35 types of hypothetical three-dimensional joint network models were constructed, and their generalised RQD values (with different thresholds) and  $MB_i$  values were measured. The correlation between the standard ratings of  $MB_i$  and RQD was assessed; based on this correlation, the theoretical RQD values of the 35 models were derived. The reasonable thresholds of the generalised RQD were determined according to the theoretical RQD values, and the optimal threshold of generalised RQD was obtained using the variation coefficient and anisotropy index of the jointing degree. The discrepancy between the results produced using traditional and generalised RQDs was discussed. Finally, an actual case study was conducted, and the results indicate that the generalised RQD associated with the optimal threshold determined in this study can properly quantify the degree of jointing of a given rock mass.

## 1. Introduction

A rock mass is a natural substance that is composed of different compositions and complex structures produced by geologic processes. It varies with the evolution of the geological environment. Owing to the complicity and invisibility of the rock mass structure, engineers cannot deeply understand the mechanical behaviour of jointed rock mass. Rock mass is separated into blocks because of the presence of joints; therefore, the mechanical properties and stabilities of engineering rock masses are deteriorated significantly [1].

Rock quality designation (RQD) [2] is a critical index to quantify the degree of jointing and is typically applied in various rock engineering worldwide, including hydraulic engineering, underground and surface mining, and rock

tunnel; furthermore, RQD has been used for over 50 years. RQD is defined as a percentage of the drill core in lengths of 100 mm or greater. Although the RQD is routinely used in practices, this concept has several inherent limitations; for example, the RQD index only considers core pieces longer than 100 mm and may result in a final RQD value that does not agree with the practice [3].

To improve the utility of the RQD, some investigations were undertaken; for example, Sen and Elssa [4] proposed the concept of volumetric RQD and evaluated the correlations between RQDs with different thresholds, volumetric joint count ( $J_v$ ), and block size; they outlined that the relations between the RQD values with different thresholds and the  $J_v$  values should be nonlinear, and such relations vary with the shapes of the blocks. Harrison [5]

reported that, with an optimal threshold, the variation in RQD values in different directions is maximal; that is, the anisotropy of the rock mass structure is highlighted maximally; additionally, through theoretical derivation, he provided a determination equation of the optimal threshold in conjunction with the maximum and minimum joint frequencies. Xu et al. [6] investigated the correlation between the fractal dimensions of joints and RQD values based on the discrete fracture network (DFN) technique. They also reported that when the rock masses are sparsely jointed, the use of traditional RQD cannot sufficiently differentiate the rock mass structures; however, when the slopes of the curve (fractal dimensions vs. RQDs with different thresholds) attain a maximum value, the associated threshold can be deemed an optimal value. Zhang et al. [7, 8] developed a determination method of the optimal RQD threshold based on a three-dimensional joint network model and setting virtual scanlines; they also claimed that the variation in RQD values can be maximised with an optimal threshold.

The reviewed literatures reported that when the RQD values are accompanied by an optimal threshold in a given rock mass, the anisotropy of the rock mass structure can be fully reflected; that is, the difference between the maximum RQD value ( $RQD_{max}$ ) and the minimum RQD value ( $RQD_{min}$ ) is maximised. However, from the perspective of engineering practicability, the RQD values accompanied by an optimal threshold should exactly quantify the degree of jointing to lay the groundwork for the subsequent tasks, e.g., rock mass quality classification and rock mass stability assessment.

Recently, the modified blockiness index ( $MB_i$ ) [9, 10] was developed as a three-dimensional measurement for the degree of rock mass jointing; using this index, the implications of blocks of different sizes on the rock mass jointing can be considered. However, the typical practice in rock engineering applications is to use RQD to quantify the degree of jointing; meanwhile, knowing the RQD value is crucial in many rock mass quality classifications and stability assessment systems, such as the rock mass rating system [11], Q-system [12], and  $Q_{slope}$ -system [13, 14]; furthermore, the associated empirical relation with the determination of support schemes has been well developed. Therefore, we do not attempt to replace the RQD with  $MB_i$  but to enhance the utility of RQD. In this study, referring to the  $MB_i$ , the determination of the optimal threshold of RQD was investigated based on the three-dimensional joint network modelling suggested by Zhang et al. [8], which can avoid the high uncertainty of the determination of RQD values. The goal of this study is to obtain an RQD value with the optimal threshold to quantify the degree of jointing more properly. Additionally, this work may provide an appropriate reference for determining a proper RQD value in other rock engineering projects.

## 2. Modified Blockiness Index ( $MB_i$ )

The block percentage ( $B$ ) [9] is defined as the ratio of the volume of blocks fully enclosed by joints to the total rock

mass volume, which ranges from 0 to 100%, and can be expressed as

$$B = \frac{\sum_{i=1}^n v_i}{V}, \quad (1)$$

where  $v_i$  is the volume of block  $i$ ,  $n$  is the number of blocks, and  $V$  is the total rock mass volume.

When the block percentage is used to quantify the degree of jointing, the effect of block size may be ignored. To address this problem, Chen et al. [10] developed the  $MB_i$ , in which the rock blocks are grouped into five categories according to block volume: 0–0.008 m<sup>3</sup>, 0.008–0.03 m<sup>3</sup>, 0.03–0.2 m<sup>3</sup>, 0.2–1.0 m<sup>3</sup>, and >1.0 m<sup>3</sup>, and the percentages of blocks in different categories are assigned different weights, i.e., the coefficients of rock block scale effect [15, 16]. The  $MB_i$  value can be calculated by

$$MB_i = B_1 + \frac{1}{2}B_2 + \frac{1}{3}B_3 + \frac{1}{4}B_4 + \frac{1}{5}B_5, \quad (2)$$

where  $B_1, B_2, B_3, B_4$ , and  $B_5$  are the block percentages of the volumes in the five intervals (0–0.008 m<sup>3</sup>, 0.008–0.03 m<sup>3</sup>, 0.03–0.2 m<sup>3</sup>, 0.2–1.0 m<sup>3</sup>, and >1.0 m<sup>3</sup>, respectively). Apparently, with an increase in the degree of jointing, the  $MB_i$  value increases and the number of small blocks inside the rock mass increases, and vice versa. The calculation of  $MB_i$  is based entirely on the three-dimensional joint network model, and this kind of model can be created by probabilistic and/or deterministic joints.

In this study, the block percentages and  $MB_i$  values were determined using the GeneralBlock program [9], in the following steps: (1) construct a three-dimensional joint network model, (2) calculate the volumes of the rock blocks that are separated by joints, and (3) determine the block percentages and  $MB_i$  values based on Eqs. (1) and (2).

## 3. Traditional and Generalised RQDs

**3.1. Traditional RQD.** Traditional RQD was pioneered by Deere in 1967 [2] and is defined by a percentage of the drill core in lengths of 100 mm or greater. The RQD concept is widely used worldwide; however, it suffers from critiques [17, 18], including the following: (i) the RQD value is anisotropic and orientation dependent and (ii) the RQD concept only considers core pieces longer than 100 mm; that is, the block scale effect is ignored.

**3.2. Generalised RQD.** The concept of generalised RQD ( $RQD_t$ ) was introduced in [7, 8]. Using this concept, the threshold can be varied. Far less work has been performed on investigating  $RQD_t$ ; however, the  $RQD_t$  is important in the investigation of the anisotropy of the rock mass structure; that is, a specified threshold can enhance the variation in  $RQD_t$  values. When the joint density is extremely high, the calculated  $RQD_t$  values in all directions are always close to 100% if the selected threshold is small; if the threshold is large, the  $RQD_t$  values will be approximately 0% regardless of the directions of the scanlines. The  $RQD_t$  value is

influenced by the threshold  $t$ , and the core pieces should be counted if their lengths are equal to or greater than  $t$ . The  $RQD_t$  can be calculated by

$$RQD_t = \frac{100}{L} \sum_{i=1}^n x_i (\%), \quad (3)$$

where  $x_i$  is the length of the core piece longer than  $t$  and  $L$  is the total length of the scanline. Given various  $t$  values, a series of  $RQD_t$  values can be obtained and subsequently used to describe the degree of jointing.

According to the recommendation from Zhang et al. [8], a calculation model of  $RQD_t$  termed "Model A-A-S" was employed, which can be expressed as follows:

$$RQD_t = \begin{cases} \frac{l_1 + l_2 + l_t}{l} \times 100\%, & (l_1 + l_2 < t), \\ \frac{l_t}{l} \times 100\%, & (l_1 + l_2 > t), \end{cases} \quad (4)$$

where  $l_1$  and  $l_2$  are the lengths of the core pieces at the start and end of the scanline, respectively, and  $l_t$  is the total length of the inner core pieces that is greater than the given threshold  $t$ .

#### 4. Development of 35 Three-Dimensional Joint Network Models and Their $MB_i$ and $RQD$ Values

**4.1. Establishment of the Hypothetical Three-Dimensional Joint Network Models.** According to the standard classification of rock joints suggested by the International Society for Rock Mechanics [19], five representative joint persistence values and seven representative joint spacing values were selected, as shown in Table 1. Additionally, the Baecher disc model [20] was applied to create the joints; it can be generated by the following parameters: the centre coordinate  $(x_0, y_0, z_0)$ , diameter  $d$ , dip direction  $\alpha$ , and dip angle  $\beta$  (Figure 1). A Baecher disc model can be represented as follows:

$$A(x - x_0) + B(y - y_0) + C(z - z_0) = 0, \quad (5)$$

$$(x - x_0)^2 + (y - y_0)^2 + (z - z_0)^2 = r = \frac{d}{2}, \quad (6)$$

where  $A = \sin \alpha \sin \beta$ ,  $B = \sin \alpha \cos \beta$ , and  $C = \cos \alpha$ . Therefore, the normal vector of the disc joint  $\mathbf{n}$  is  $(A, B, C)$ .

The orientations of the joints were assumed to exhibit a Fisher distribution:

$$f(\alpha, \beta) = f(\beta)f(\alpha) = \frac{1}{2\pi} \frac{\kappa \sin \alpha}{2 \sinh \kappa} e^{\kappa \cos \alpha}, \quad (7)$$

where  $\kappa$  is the Fisher coefficient. In addition, the three-dimensional density of a set of joints can be determined by

$$d_3 = \frac{4d_1}{\pi E(D^2)E(|n \cdot i|)}, \quad (8)$$

where  $i$  is the vector along the scanline  $l$  and  $E(D^2)$  is the mean value of the squared joint diameter.

When the number of joint sets is constant, the joint density/frequency/spacing affects the degree of rock mass jointing the most, followed by joint persistence [11, 21]; meanwhile, other geometrical parameters, such as joint orientation and distribution type, have negligible influences on such a degree [22]. The number of joint sets was fixed to three in this study, and other geometrical parameters of joints (with the exceptions of joint spacing and persistence) were also unchanged (Table 2), because (1) blocks form inside the rock mass as three sets of joints exist and (2) the computing time is always dissatisfactory if the number of joint sets is larger than three. The selected five representative joint persistence values and seven representative joint spacing values were cross-joined; hence, 35 pairs of "persistence-spacing" were obtained. Additionally, based on Eq. (8) and Table 2, the three-dimensional joint density of each pair was calculated, as shown in Table 3.

The flow chart to show the process of generating the network model is shown in Figure 2. Based on Tables 2 and 3, 35 types of hypothetical three-dimensional joint network models were constructed, as shown in Figure 3. It is noteworthy that the sizes of all models arrive at the geometrical representative elementary volume of rock mass [23].

**4.2.  $MB_i$  Values of All Models.** The blocks inside the 35 models and their volumes were identified; after removing the blocks formed by a combination of the boundary surfaces and joints, the  $MB_i$  values of all models were measured using Eq. (2); these values are presented in Table 4. The table shows that the wider the joint spacing is, the smaller the  $MB_i$  value is; also, the higher the joint persistence is, the larger the  $MB_i$  value is.

**4.3. Measurement of  $RQD_t$  Values.** Referring to the associated definition, the  $RQD_t$  values of a three-dimensional joint network model were measured by setting the scanlines. Three cross sections were extracted along the plane at  $1/2L_x$ ,  $1/2L_y$ , and  $1/2L_z$  ( $L_x$ ,  $L_y$ , and  $L_z$  mean the lengths of the sides in the X, Y, and Z directions, respectively), and scanlines were established through the geometrical centre of the cross sections every  $10^\circ$ , as illustrated in Figure 4. Hence, a total of 18 or 54 scanlines were set in the cross section or on the model.

When the cross section is extracted at  $1/2L_x$ , the scanline can be expressed as

$$\begin{cases} x_s = \frac{1}{2}L_x, \\ z_s = y_s \cdot \tan\left|\frac{\pi}{2} - \beta_s\right|, \end{cases} \quad (9)$$

where  $\beta_s$  is the plunge of a scanline.

From Eqs. (5), (6), and (9), an equation of the intersection of the joint and scanline can be established; if the solution of this equation is a real number, the intersection point between the joint and scanline exists, and vice versa. After the coordinates of the intersection points are

TABLE 1: Selected representative values of joint spacing and persistence.

Joint spacing classification	Extremely wide	Very wide	Wide	Moderate	Close	Very close	Extremely close
Selected value (m)	6	4	1.3	0.4	0.13	0.04	0.02
Joint persistence classification	Very high	High	Medium	Low	Very low		
Selected value (m)	40	20	10	3	1		

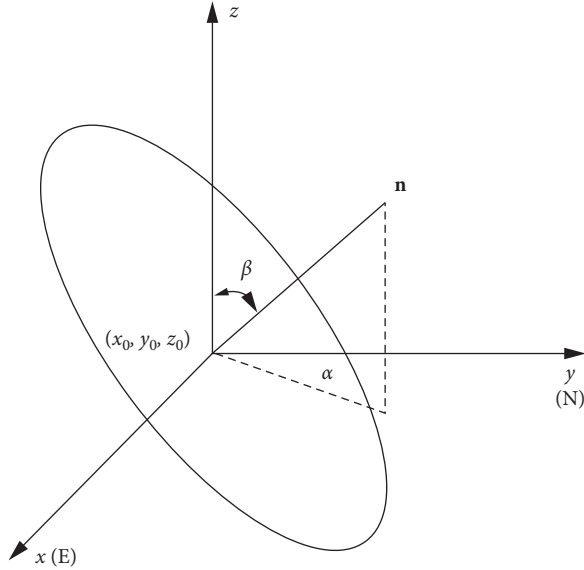
FIGURE 1: Disc model of the joint.  $\mathbf{n}$  is the normal vector of the disc joint.

TABLE 2: Distribution parameters of the joint parameters of the theoretical DFN model.

Joint set no.	Set 1	Set 2	Set 3
Distribution type of joint persistence	Uniform	Uniform	Uniform
Distribution type of joint orientation	Uniform	Uniform	Uniform
Fisher's coefficient $\kappa$	0	0	0
Average dip direction/dip angle ( $^\circ$ )	0/90	90/0	90/90

determined, the length of the core piece along the scanline can be calculated.

Using the aforementioned measurement of the core piece length, a total of 54  $RQD_t$  values can be determined in the model, and the mean can be regarded as the representative  $RQD_t$  value of this model. When the investigation of the optimal  $t$  value of  $RQD_t$  is implemented, a series of  $g$   $RQD_t$  values can be calculated with the variation in the  $t$  value.

## 5. Investigation of Selecting an Optimal Threshold of $RQD_t$

**5.1. Correlation between the Standard Ratings of  $MB_i$  and  $RQD$ .** The  $MB_i$  and  $RQD$  indices can be used to quantify the degree of rock mass jointing, and both of them divide such a degree into five categories, as shown in Tables 5 and 6. The

correlation between standard ratings of  $MB_i$  and  $RQD$  was assessed; this is shown in Figure 5. From this figure, a good linear relation was found between the standard ratings of  $MB_i$  and  $RQD$ , which is expressed as

$$RQD = 100 - 0.92MB_i. \quad (10)$$

The determination coefficient is 0.99, indicating a high fitting degree. Based on Eq. (10), theoretical  $RQD$  values can be derived.

**5.2. Theoretical  $RQD$  Values.** From Table 4 and Eq. (10), the theoretical  $RQD$  values of the 35 models were determined, as shown in Table 7. The theoretical  $RQD$  value can be defined as an  $RQD$  value derived by the  $MB_i$ , which is more compatible with the actual degree of rock mass jointing.

**5.3. Selection of Optimal Threshold of  $RQD_t$ .** The three-dimensional joint network model with a joint persistence of 20 m and joint spacing of 1.3 m was used as an example to demonstrate the procedure for selecting an optimal threshold of the  $RQD_t$ . Based on the measurement described in Section 4.3, the (representative)  $RQD_t$  values of different thresholds were calculated, as shown in Figure 6. The figure indicates that (1) when the threshold is 100 mm, the  $RQD_t$  value is close to 100%, and when the threshold is 1000 mm, the  $RQD_t$  value is approximately 70%, and (2) with the increase in  $t$  value, the  $RQD_t$  values tend to be reduced.

As shown in Table 4, the  $MB_i$  value of this example model is 13.50%, which belongs to Class II ("relatively integrated" category). The corresponding rating of the theoretical  $RQD$  value also belongs to Class II ("good" category); that is, when the measured  $RQD_t$  values are in the interval of 75% to 90%, the  $RQD_t$  values can be regarded as reasonable, and the corresponding  $t$  values can be termed as reasonable thresholds.

Figure 6 shows that the reasonable thresholds are 600 mm, 700 mm, 800 mm, and 900 mm, and an optimal  $t$  value should be further selected. Owing to the anisotropy of the rock mass structure, the  $RQD_t$  values in different directions are varied. To reflect the anisotropy of rock mass clearly, the variation in the  $RQD_t$  values with an optimal  $t$  value should be maximised. Therefore, the variation coefficient ( $C_{v-RQD}$ ) and anisotropy index of jointing degree ( $AI_{jd}$ ) [24] were introduced to measure the dispersion of the  $RQD_t$  values with the same threshold but at different directions. The  $C_{v-RQD}$  and  $AI_{jd}$  are two different indices that share a common feature in that when the  $RQD_t$  values in different directions are dispersed, both the  $C_{v-RQD}$  and  $AI_{jd}$  values are relatively large, and vice versa. The  $C_{v-RQD}$  can be calculated by

TABLE 3: Three-dimensional joint densities of 35 pairs of “persistence-spacing.”

Joint persistence (m)		Joint spacing (m)						
		Extremely wide 0.02	Very wide 0.04	Wide 0.13	Moderate 0.4	Close 1.3	Very close 4	Extremely close 6
40	Very high	0.0398	0.0199	0.0061	0.0020	0.0006	0.0002	0.0001
20	High	0.1592	0.0796	0.0245	0.0080	0.0024	0.0008	0.0005
10	Medium	0.6369	0.3185	0.9799	0.0318	0.0098	0.0032	0.0021
3	Low	7.0771	3.5386	1.0888	0.3539	0.1089	0.0354	0.0236
1	Very low	63.6620	31.8310	9.7942	3.1831	0.9794	0.3183	0.2122

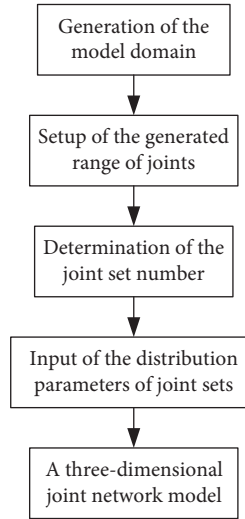


FIGURE 2: Flow chart of the generation of a three-dimensional joint network model.

$$C_{v-RQD} = \frac{\sigma_{RQD}}{\mu_{RQD}}, \quad (11)$$

where  $\sigma_{RQD}$  and  $\mu_{RQD}$  are the standard deviation and mean of the measured  $RQD_t$  values in a model, respectively. The  $AI_{jd}$  can be expressed as

$$AI_{jd} = RQD_{t_{max}} \frac{RQD_{t_{max}} - RQD_{t_{min}}}{100}, \quad (12)$$

where  $RQD_{t_{max}}$  and  $RQD_{t_{min}}$  are the maximum and minimum  $RQD_t$  values, respectively.

For the three-dimensional joint network model exemplified in this section, the reasonable  $t$  values are 600 mm, 700 mm, 800 mm, and 900 mm. To select the optimal threshold, the  $C_{v-RQD}$  and  $AI_{jd}$  of  $RQD_t$  values with the four thresholds were calculated, as shown in Figure 7. The figure presents a tendency that the  $C_{v-RQD}$  and  $AI_{jd}$  increase with the increasing threshold. Meanwhile, all the  $C_{v-RQD}$  values are greater than 0.1, indicating strong variation degrees. As the threshold is 900 mm, the  $C_{v-RQD}$  and  $AI_{jd}$  values are the highest, implying that the  $RQD_t$  values with a threshold of 900 mm can fully reflect the anisotropy of the rock mass structure. Thus, the optimal threshold is 900 mm.

The optimal thresholds of all models were determined, as shown in Table 8. A review of Table 8 indicates that when the joint persistence is 3 m or more, the optimal  $t$  values first increase and subsequently decrease with the increase in joint spacing; for example, when the joint persistence

remains unaltered as 40 m, the optimal  $t$  value increases from 200 mm to 800 mm and subsequently decreases to 100 mm. This can be attributed to two factors: (1) the wider the joint spacing is, the more integrated the rock mass is and the smaller the variation in the  $RQD_t$  values is, and (2) with the increasing joint spacing, the variation in the  $RQD_t$  values tends to be increasingly smaller regardless of the change in  $t$  value; particularly, when joint persistence is very wide or extremely wide, the  $RQD_t$  values change little or not at all because all the corresponding  $C_{v-RQD}$  and  $AI_{jd}$  values are extremely low. Hence, the  $RQD_t$  values with a  $t$  value of 100 mm are enough to accurately describe those rock masses sparsely jointed or integrated. Additionally, when the joint spacing is unchanged, the change in joint persistence appears to have minor effects on the determination of the optimal  $t$  value; for example, when the joint spacing is fixed at 0.4 m, the optimal  $t$  values vary irregularly, and when the joint spacing is fixed as 6 m, the optimal  $t$  values do not change. It can be concluded that the major determinant factor for selecting the optimal  $t$  value is joint spacing.

## 6. Comparative Analysis of Traditional and Generalised RQDs

To evaluate the difference between traditional and generalised RQDs, the scatter plots of traditional and generalised RQDs and  $MB_i$  values are shown in Figure 8, and the

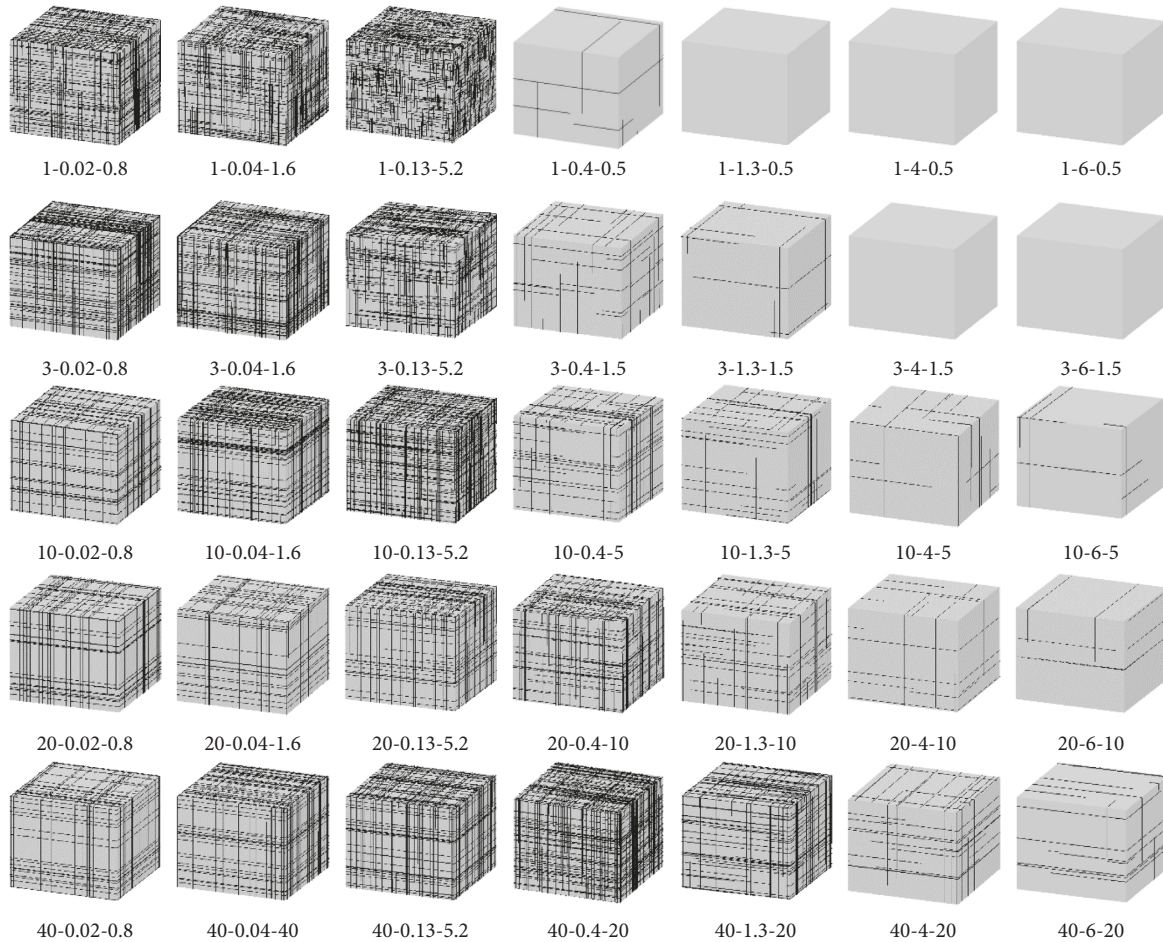


FIGURE 3: Thirty-five types of three-dimensional joint network models with different combinations of joint spacing and persistence. Each model's number is stated below the model; the first number indicates joint persistence, the second indicates joint spacing, and the third represents the side length of the model.

TABLE 4:  $MB_i$  values (%) of the 35 types of hypothetical models and the corresponding ratings.

Joint persistence (m)		Joint spacing (m)						
		Extremely wide 0.02	Very wide 0.04	Wide 0.13	Moderate 0.4	Close 1.3	Very close 4	Extremely close 6
40	Very high	93.7571	91.4286	61.2567	27.5231	17.5350	10.5002	0.3650
20	High	91.0728	87.5613	44.6782	23.9566	13.5002	0.3186	0.0307
10	Medium	90.2910	87.2045	44.0021	20.9621	4.6818	0.0573	0.0012
3	Low	88.9321	86.0180	43.8025	7.9657	0.1070	1.20E-8	1.78E-10
1	Very low	87.9759	84.3504	18.2843	0.1110	5.13E-5	1.03E-7	1.74E-9

corresponding cumulative frequency curves are presented in Figure 9.

As shown in Figure 8, when the rock mass is integrated (i.e., the  $MB_i$  value ranges from 0 to 7%), the generalised RQD values are almost consistent with the traditional RQD values. However, when the rock mass is in Class II ("relatively integrated" category) or lower, significant discrepancies between traditional and generalised RQD values appear, and the general tendency is that the generalised RQD values are less than the traditional RQD values. A model of  $y = 100 - x$  was adopted to fit the two kinds of data points in Figure 8; as shown, the fitting degree of the data points in

generalised RQD vs.  $MB_i$  is better than that of the data points in traditional RQD vs.  $MB_i$ ; especially in the  $MB_i$  interval of 85% to 100%, it indicates fractured rock masses, but the traditional RQD values range from Classes III to V ("fair" to "very poor" category). This suggests that the traditional RQD values may mismatch with the  $MB_i$  values that are three-dimensional quantifications of the rock mass jointing degree. Obviously, the generalised RQD values with optimal thresholds perform better in this aspect because the fitting degree of the generalised RQD and  $MB_i$  values is rather high, and the RQD's ability to differentiate rock mass structures is similar to that of the  $MB_i$ .

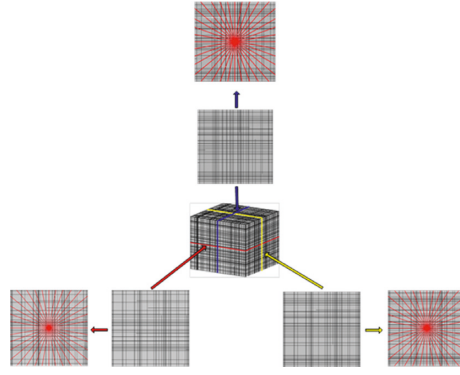


FIGURE 4: Illustration of setting scanlines in a model.

TABLE 5: Standard ratings of  $MB_i$ .

$MB_i$	<7	7–27	27–55	55–85	$\geq 85$
Rating	I	II	III	IV	V
Description	Integrated	Relatively integrated	Poorly integrated	Relatively fractured	Fractured

TABLE 6: Standard ratings of RQD.

RQD	90–100	75–90	50–75	25–50	<25
Rating	I	II	III	IV	V
Description	Very good	Good	Fair	Poor	Very poor

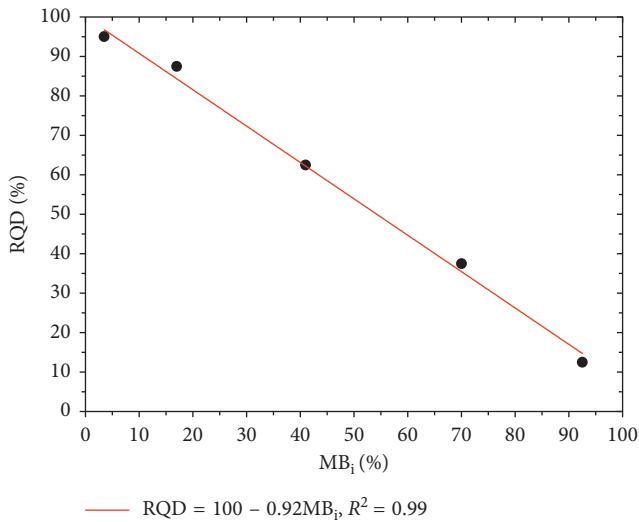


FIGURE 5: Correlation between the standard ratings of  $MB_i$  and RQD.

In Figure 9, the cumulative frequency curve of the generalised RQD is below that of the traditional RQD; that is, the curve of the generalised RQD attains 100% later, implying that the ability of the generalised RQD to distinguish rock mass structures is superior, as shown in Figure 8: the data points (generalised RQD vs.  $MB_i$ ) distribute evenly on both sides of the fitting line of  $y = 100 - x$ . However, for the three-dimensional joint network models with similar  $MB_i$  values, the acquired traditional RQD values range widely, as shown in Figure 8.

## 7. Engineering Practice

The investigation of the optimal threshold of generalised RQD was performed based on the joint data gathered on the dam rock mass in the Zipingpu hydropower station (Figure 10), Sichuan, China. The analysis of the joint data identifies three joint sets, and their probabilistic distribution parameters are presented in Table 9. Based on Table 9, a three-dimensional joint network model of the dam rock mass was constructed, as shown in Figure 11. Using the procedure for determining the  $RQD_t$  values described in Section 4.3, the generalised RQD values with different thresholds and directions were measured (Figure 12), and their means were calculated (Table 10). Table 10 shows that the traditional RQD value is 96.95%, which is in Class I (“good” category). The blocks inside the three-dimensional joint network model and their volumes were identified, and the  $MB_i$  value of this model was determined to be 17%, which belongs to Class II (“relatively integrated” category).

As shown in Figure 11, the traditional RQD values (in different directions) are almost in proximity to 100%, which cannot highlight the anisotropy of the rock mass structure; however, the increase in threshold resulted in an improvement; that is, in the polar coordinate (Figure 12), the contours that indicate the  $RQD_t$  values with the same threshold but different directions are elliptical or bow-tie-shaped if the threshold is equal to or greater than 200 mm.

Additionally, Table 10 presents the average  $RQD_t$  values with different thresholds; clearly, the traditional RQD value

TABLE 7: Theoretical RQD values (%) of all hypothetical models.

Joint persistence (m)		Joint spacing (m)						
		Extremely wide 0.02	Very wide 0.04	Wide 0.13	Moderate 0.4	Close 1.3	Very close 4	Extremely close 6
40	Very high	11.50	13.69	42.03	73.71	83.08	89.69	99.21
20	High	14.03	17.32	57.59	77.05	86.87	99.25	99.52
10	Medium	14.76	17.66	58.23	79.87	95.16	99.55	99.55
3	Low	16.04	18.78	58.42	92.07	99.45	99.55	99.55
1	Very low	16.94	20.34	82.39	99.45	99.55	99.55	99.55

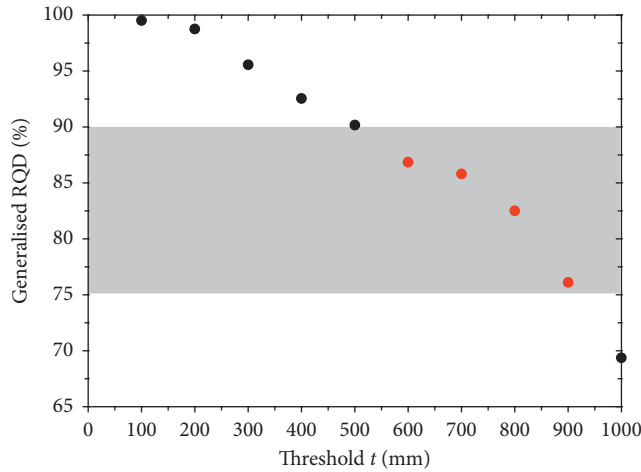


FIGURE 6: Generalised RQD values with different thresholds of the exemplified model.

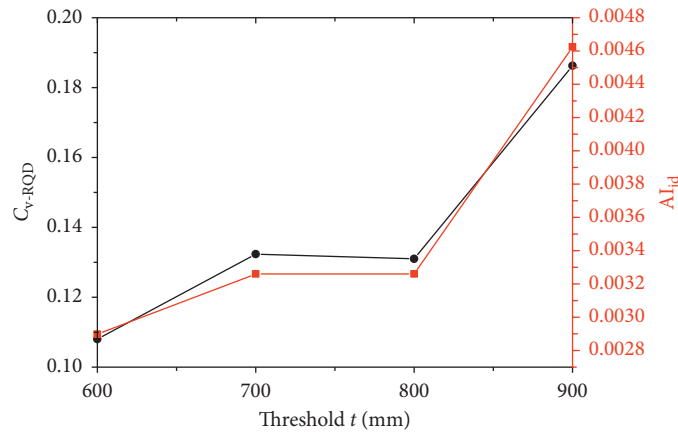


FIGURE 7:  $C_{v-RQD}$  and  $AI_{jd}$  of the  $RQD_t$  values with reasonable thresholds.

is slightly unreasonable and cannot correspond to the  $MB_i$  value. Based on the method described in Section 5, the reasonable  $t$  value was determined to be 200 mm; therefore, an optimal threshold of 200 mm was obtained directly. Therefore, as shown in Table 10, the corresponding generalised RQD value is 75.45%, which is in Class II (“good” category) and consistent with the measured  $MB_i$  value.

### 8. Conclusions

- (1) A total of 35 types of hypothetical three-dimensional joint network models were established, their

generalised RQD values with different thresholds were measured, and a procedure for determining the optimal threshold of RQD was developed. This procedure was based on the  $MB_i$ ; if the measured generalised RQD values are consistent with the  $MB_i$  with respect to the rating of the rock mass jointing degree, the corresponding thresholds are regarded as reasonable thresholds; subsequently, using the  $C_{v-RQD}$  and  $AI_{jd}$ , an optimal threshold was determined.

- (2) The comparison between the traditional RQD values and the generalised RQD values with optimal thresholds indicated that (1) when the rock masses

TABLE 8: Optimal thresholds of all hypothetical models.

Joint persistence (m)		Joint spacing (m)						
		Extremely wide 0.02	Very wide 0.04	Wide 0.13	Moderate 0.4	Close 1.3	Very close 4	Extremely close 6
40	Very high	200	200	300	500	800	100	100
20	High	100	300	200	200	900	100	100
10	Medium	100	100	100	300	100	100	100
3	Low	100	200	200	300	100	100	100
1	Very low	100	100	100	100	100	100	100

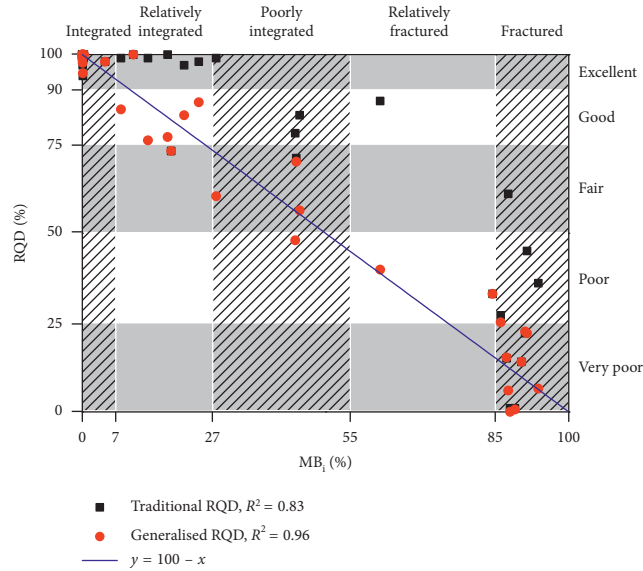


FIGURE 8: Scatter plot of traditional and generalised RQDs and  $MB_i$  values.

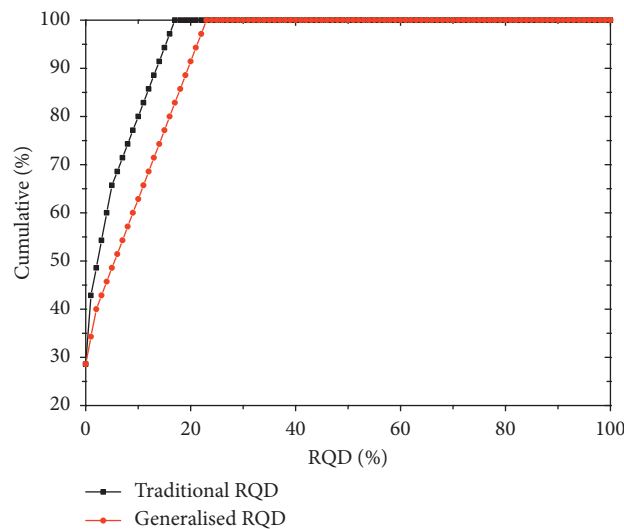


FIGURE 9: Comparison between the cumulative frequency curves of traditional and generalised RQDs.

were integrated (rated in  $MB_i$ ), the measured traditional RQD values were similar to the generalised RQD values; (2) when the degrees of rock mass jointing were in Class II (“relatively integrated” category in  $MB_i$ ) or poorer, significant differences

were found between the measured traditional and generalised RQD values; and (3) the traditional RQD may fail to differentiate rock masses possessing various structures, and the generalised RQD was superior (as shown in Figures 8 and 9).



FIGURE 10: Zipingpu hydropower station in Sichuan, China.

TABLE 9: Joint data of the dam rock mass.

Joint set no.	Joint number	Joint orientation			Trace length		$d_3$ ( $m^{-3}$ )
		Dip direction ( $^{\circ}$ )	Dip angle ( $^{\circ}$ )	Fisher's coefficient $\kappa$	Distribution type	Average trace length	
1	20	75	64	7.38	Lognormal	10	0.024
2	10	5	85	5.95	Lognormal	7	0.012
3	20	33	49	5.73	Lognormal	7	0.025

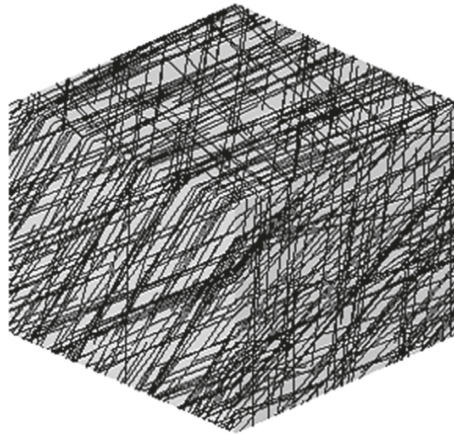


FIGURE 11: Three-dimensional joint network model of the dam rock mass.

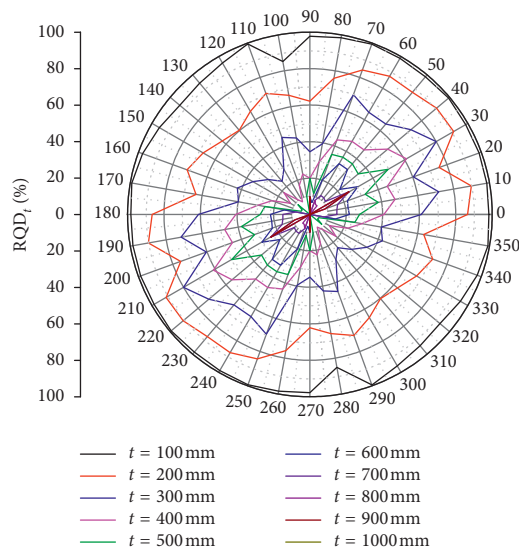


FIGURE 12: Generalised RQD values (in different directions) with various thresholds of the dam rock mass.

TABLE 10: Average generalised RQD values with different thresholds of the dam rock mass.

$t$ (mm)	100	200	300	400	500	600	700	800	900	1000
$RQD_t$	96.96	75.45	50.32	31.95	20.81	12.86	7.30	3.55	2.40	0.00

- (3) The investigation of selecting an optimal threshold of  $RQD_t$  was conducted based on an actual jointed rock mass, and the result indicated that the generalised  $RQD$  value with an optimal threshold could properly quantify the jointing degree of a real rock mass compared to  $MB_i$ , when using the procedure developed in this study.

## Data Availability

The data used to support the findings of this study are available from the corresponding author upon request.

## Conflicts of Interest

The authors declare that there are no conflicts of interest regarding the publication of this paper.

## Authors' Contributions

All authors contributed equally to this work.

## Acknowledgments

This work was financially supported by the National Science Foundation for Young Scientists of China (grant number 41402306) and the Open Research Fund of State Key Laboratory of Geomechanics and Geotechnical Engineering, Institute of Rock and Soil Mechanics, Chinese Academy of Sciences (grant number Z016015).

## References

- [1] F. Agliardi, G. B. Crosta, F. Meloni, C. Valle, and C. Rivolta, "Structurally-controlled instability, damage and slope failure in a porphyry rock mass," *Tectonophysics*, vol. 605, pp. 34–47, 2013.
- [2] D. U. Deer, A. J. Hendron, F. D. Patton, and E. J. Cording, "Design of Surface and Near-Surface Construction in Rock," in *Failure and Breakage of Rock*, C. Fairhurst, Ed., pp. 237–302, Society of Mining Engineers of AIME, New York, NY, USA, 1967.
- [3] R. Bertuzzi, K. Douglas, and G. Mostyn, "Comparison of quantified and chart GSI for four rock masses," *Engineering Geology*, vol. 202, pp. 24–35, 2016.
- [4] Z. Sen and E. A. Eissa, "Volumetric rock quality designation," *Journal of Geotechnical Engineering*, vol. 117, no. 9, pp. 1331–1346, 1991.
- [5] J. P. Harrison, "Selection of the threshold value in RQD assessments," *International Journal of Rock Mechanics and Mining Sciences*, vol. 36, no. 5, pp. 673–685, 1999.
- [6] L. Xu, Q. Wang, J. Chen, F. Zhou, and C. Tan, "Study of correlation between fractal dimension and RQD of three-dimensional jointed rock mass," *Chinese Journal of Rock Mechanics and Engineering*, vol. 30, no. 1, pp. 2667–2674, 2011, in Chinese.
- [7] W. Zhang, Q. Wang, J.-p. Chen, C. Tan, X.-q. Yuan, and F.-j. Zhou, "Determination of the optimal threshold and length measurements for RQD calculations," *International Journal of Rock Mechanics and Mining Sciences*, vol. 51, pp. 1–12, 2012.
- [8] W. Zhang, J. Chen, Q. Wang, D. Ma, C. Niu, and W. Zhang, "Investigation of RQD variation with scanline length and optimal threshold based on three-dimensional fracture network modeling," *Science China Technological Sciences*, vol. 56, no. 3, pp. 739–748, 2013.
- [9] L. Xia, M. Li, Y. Chen, Y. Zheng, and Q. Yu, "Blockiness level of rock mass around underground powerhouse of Three Gorges Project," *Tunnelling and Underground Space Technology*, vol. 48, pp. 67–76, 2015.
- [10] Q. Chen, W. Niu, W. Zheng, J. Liu, T. Yin, and Q. Fan, "Correction of some problems in blockiness evaluation method in fractured rock mass," *Rock and Soil Mechanics*, vol. 39, no. 7, pp. 1–8, 2018, in Chinese, <http://kns.cnki.net/kcms/detail/42.1199.O3.20180413.1118.003.html>.
- [11] Z. T. Bieniawski, *Engineering Rock Mass Classifications*, Wiley, New York, NY, USA, 1989.
- [12] N. Barton, R. Lien, and J. Lunde, "Engineering classification of rock masses for the design of tunnel support," *Rock Mechanics Felsmechanik Mécanique des Roches*, vol. 6, no. 4, pp. 189–236, 1974.
- [13] N. Bar and N. Barton, "The Q-slope method for rock slope engineering," *Rock Mechanics and Rock Engineering*, vol. 50, no. 12, pp. 3307–3322, 2017.
- [14] N. Bar and N. Barton, "Rock slope design using Q-slope and geophysical survey data," *Periodica Polytechnica Civil Engineering*, vol. 62, no. 4, pp. 893–900, 2018.
- [15] D. J. Chen and H. T. Liu, *A New Index for Evaluating Rock Mass Qualities: Blockiness Modulus*, Chinese first selection of engineering geological academic conference papers, Soochow, China, 1979, in Chinese.
- [16] C. Y. Wang, P. L. Hu, and W. C. Sun, "Method for evaluating rock mass integrity based on borehole camera technology," *Rock and Soil Mechanics*, vol. 31, pp. 1326–1330, 2010.
- [17] A. Palmstrom, "Measurements of and correlations between block size and rock quality designation (RQD)," *Tunnelling and Underground Space Technology*, vol. 20, no. 4, pp. 362–377, 2005.
- [18] P. J. Pells, Z. T. Bieniawski, S. R. Hencher, and S. E. Pells, "Rock quality designation (RQD): time to rest in peace," *Canadian Geotechnical Journal*, vol. 54, no. 6, pp. 825–834, 2017.
- [19] ISRM, "Suggested methods for the quantitative description of discontinuities in rock masses," *International Journal of Rock Mechanics and Mining Sciences and Geomechanics Abstracts*, vol. 16, no. 2, p. 22, 1979.
- [20] G. B. Baecher, N. A. Lanney, and H. H. Einstein, "Statistical description of rock properties and sampling," in *Proceedings of 18th U.S. Symposium on Rock Mechanics*, pp. 1–8, Golden, Colorado, USA, June 1977.
- [21] B. H. Kim, M. Cai, P. K. Kaiser, and H. S. Yang, "Estimation of block sizes for rock masses with non-persistent joints," *Rock Mechanics and Rock Engineering*, vol. 40, no. 2, pp. 169–192, 2006.
- [22] Q. Zhang, Z. Bian, and M. Yu, "Preliminary research on rockmass integrity using spatial block identification technique," *Yanshilixue Yu Gongcheng Xuebao/Chinese Journal of Rock Mechanics and Engineering*, vol. 28, no. 3, pp. 507–515, 2009, in Chinese.
- [23] L. Xia, Y. Zheng, and Q. Yu, "Estimation of the REV size for blockiness of fractured rock masses," *Computers and Geotechnics*, vol. 76, pp. 83–92, 2016.
- [24] J. Zheng, X. Yang, Q. Lü, Y. Zhao, J. Deng, and Z. Ding, "A new perspective for the directivity of Rock Quality Designation (RQD) and an anisotropy index of jointing degree for rock masses," *Engineering Geology*, vol. 240, pp. 81–94, 2018.

